Seasonal Variations of the Subsurface Thermal Structure in the Gulf of Guinea[1]

ROBERT W. HOUGHTON

Lamont-Doherty Geological Observatory of Columbia University, Palisades, NY 10964

(Manuscript received 20 April 1983, in final form 18 July 1983)

ABSTRACT

The subsurface thermal structure in the Gulf of Guinea is analyzed using the historical hydrographic data file. Of particular interest is the rapid vertical displacement of the thermal structure from the warm (March–May) season to the cold (July–August) season. This displacement field is trapped at the equator with vertical and meridional scales appropriate to a second or third mode baroclinic Kelvin wave. It has a maximum amplitude between 4°W and 10°W with a node near 2°E. South of 4°S no seasonal displacement of the thermocline underlies the seasonal variation in the sea surface temperature. Along the eastern boundary north of the equator to 3°E the displacement field vanishes. Thus the coastal upwelling associated with a vertical displacement tightly bound to the northern coast from 2°E to 10°W appears detached from the equatorial regime.

1. Introduction

Sea surface temperature (SST) variations in the equatorial Atlantic are dominated by the annual signal with an amplitude of 1–2°C in the west increasing to 5–7°C in the Gulf of Guinea where the thermocline shoals and where the amplitude of the annual signal is several times greater than the interannual variability (Merle *et al.*, 1979). The spatial pattern of this annual signal is illustrated in Fig. 1 which is adapted from the climatic SST maps of Hastenrath and Lamb (1977). During the "cold season", most fully developed in July and August, cold water appears as a broad tongue extending along the equator from the eastern boundary to 30°W, separate from a narrow band of cold water along the northern boundary between 2°E and 8°W.

The origin of this cold water has been a subject of considerable debate. The SST pattern suggests that this feature results from the advection of cold coastally upwelled water by the South Equatorial Current (SEC). However, many observations suggest otherwise. First, the cold tongue often develops too rapidly for any realistic current speed (Houghton, 1981). Detailed SST analysis of METEOSAT data (Citeau *et al.*, 1981) reveals bands of warm water separating the equatorial and coastal regions that preclude any simple advective model. Finally, surface nutrient concentrations at the equator in the Gulf of Guinea (Voituriez, 1981) appear to originate from the underlying equatorial undercurrent (EUC) rather than coastally upwelled water to the east.

In the equatorial Atlantic changes in the upper thermal structure are primarily a response to wind forcing. Katz *et al.* (1977) have shown that the zonal pressure gradient in the western and central equatorial Atlantic varies almost in phase with the seasonal variation of the local wind stress. The zonal tilt of the thermocline across the entire equatorial Atlantic has been shown by Merle (1980) to be greatest during July–September and least during April–June with a "pivot" point near 25°W. The forcing mechanism responsible for this seasonal thermocline displacement, and presumably then the cold SST in the Gulf of Guinea, has been the subject of considerable research and speculation. There has been no convincing demonstration of a correlation between the cold SST and the local, primarily meridional wind (Houghton, 1976; Berrit, 1976; Bakun, 1978; Voituriez, 1981; Servain *et al.*, 1982). According to the model by Philander and Pacanowski (1981), a meridional wind stress would produce upwelling in the Gulf of Guinea south of the equator. In contrast, a response to a zonal wind stress would be trapped near the symmetric about the equator. A variety of models has been developed with various combinations of local, remote, periodic, and step-function wind forcing. We will compare these model predictions with our results in Section 4.

The objective of this paper is to describe the seasonal variation of the thermal structure throughout the Gulf of Guinea. In particular we are interested in understanding how much of the thermal structure is a response to ocean dynamic forcing. Analysis using the more numerous SST data is of limited value for this objective because air–sea fluxes of heat and advection of cold water by the SEC can obscure the SST variation that is due to change in the underlying thermal struc-

[1] Lamont-Doherty Geological Observatory Contribution Number 3538.

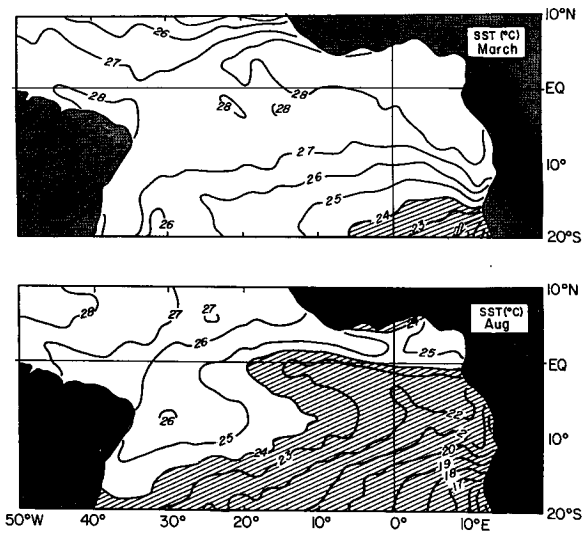

FIG. 1. Climatic averaged sea-surface temperature for March and August (adapted from Hastenrath and Lamb, 1977).

ture. Our analysis will be an extension of work by Merle (1980, 1983), but confined to the Gulf of Guinea with special attention to vertical structure and to finer spatial resolution.

In Section 2 the data set will be described. The results of our analysis will be presented in Section 3 followed by a discussion and comparison with model predictions in Section 4 and conclusions in Section 5.

2. Data

The data used in this study consist of NODC Nansen stations, edited and merged with additional MBT and XBT data from the French Navy, courtesy of Jacques Merle. The file extends to 1975 and includes GATE data. The file consists of listings at standard levels of 0, 5, 10, 20, 30, 40, 50, 60, 75, 100, 125, 150, 200, 250, 300, 400, and 500 m. The depth of a particular isotherm is calculated by a linear interpolation between these levels.

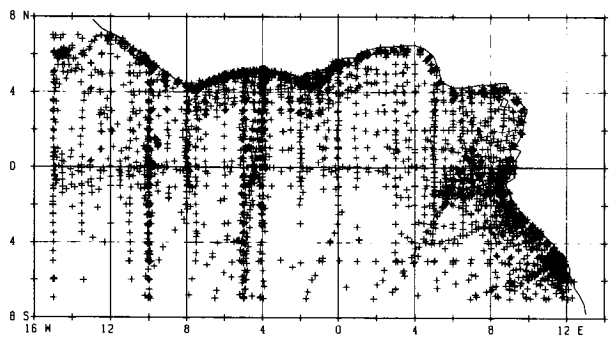

FIG. 2. Distribution of historical hydrographic data in the Gulf of Guinea.

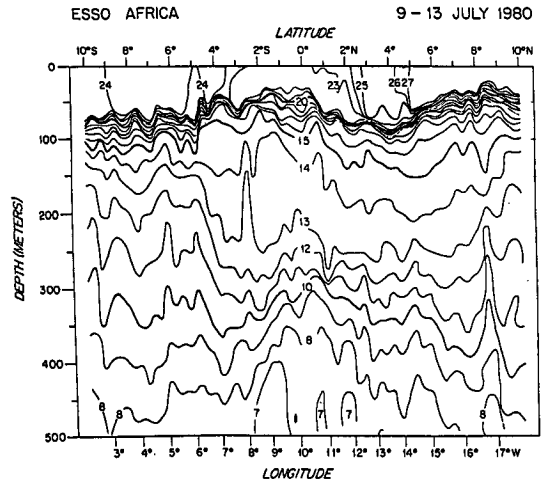

FIG. 3. Temperature section across equator on oblique line from 10°N, 18°W to 10°S, 2°W (courtesy, J. Bruce).

The data distribution is shown in Fig. 2. Within the area bounded by 15°W, 7°S and the coast there are approximately 10 000 stations. Mean monthly temperature profiles were calculated on grids 2° in longitude and 1° in latitude. We will see that this grid size is necessary to resolve the meridional structure near the equator. On average each grid point contains five stations, though the spatial distribution is very uneven. South of the equator data are sparse except along the 10°W and 4°W meridians. Our initial analysis will focus on 4°W longitude where the average is 15 stations per grid point.

3. Analysis

The objective of our analysis is to describe changes in the thermal structure of the equatorial Atlantic over the upper several hundred meters. Various parameters have been used to characterize this structure both in data analysis and numerical model calculations. The depth of the thermocline or the surface mixed-layer depth is readily compared to the interface depth of a two-layer model. Integrated quantities such as the heat content and dynamic height often give better agreement with model predictions since they average over the internal structure especially when the real ocean is not a perfect two-layer system. Instead we will calculate the depth of particular isotherms since we want to describe some of this internal structure. We will show that within the Gulf of Guinea the 20°C isotherm can be a proxy for the thermocline.

The thermal structure in the Gulf of Guinea, illustrated in Fig. 3, is characterized by a relatively shallow mixed layer, 20–50 m thick, overlying a sharp thermocline. At the equator the thermocline is broadened by the EUC. Throughout this section the 20°C isotherm is contained within the thermocline. This is not necessarily the case elsewhere in the equatorial Atlantic.

In Fig. 4 we show the depth of 20°C and the thermocline at the equator calculated from mean monthly profiles average over 5° longitude by 2° latitude. The dot denotes the depth of maximum temperature gradient and the bars the depth range over which

$$\frac{dT}{dz} > 0.1°\text{C m}^{-1}.$$

The standard deviation of the 20°C depth (solid line) is approximately 10 m. In the far west the amplitude of the seasonal thermocline displacement is greater than the 20°C displacement although the two are in phase. At times 20°C is located above or below the thermocline. Moving east we see the two curves become similar. This pattern persists into the Gulf of Guinea (east of 15°W) where the 20°C isotherm remains approximately 10 m below the maximum temperature gradient.

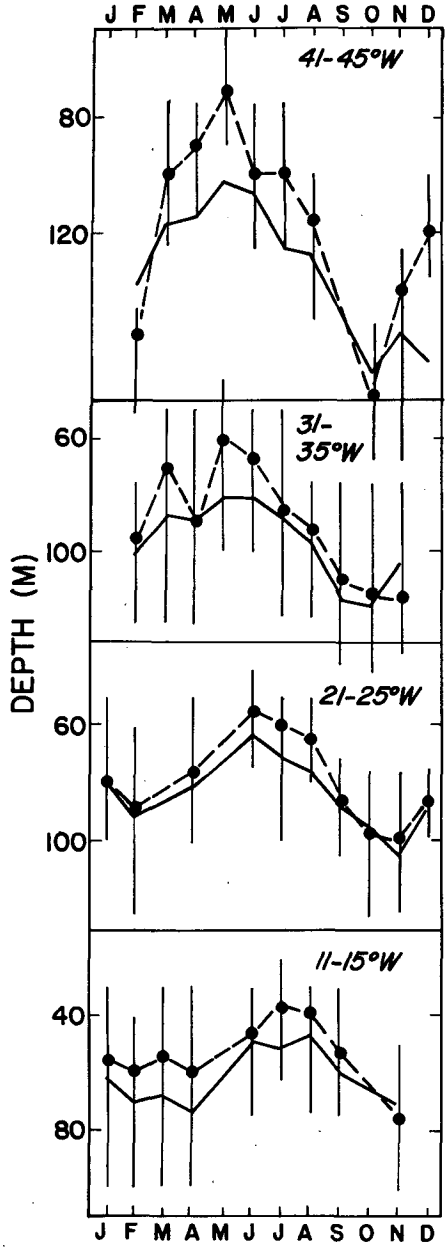

FIG. 4. Annual cycle of depth of 20°C along the equator (solid line) and the thermocline depth (dashed line). Dots show depth of maximum dT/dz and vertical bars show depth interval for which $dT/dz > 0.1°\text{C m}^{-1}$.

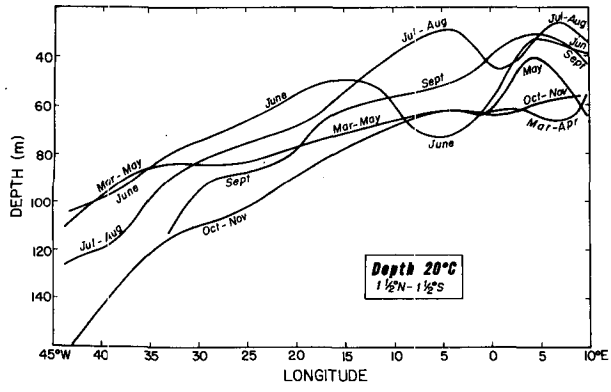

FIG. 5. Climatic average depth of 20°C between 1½°N and 1½°S. Curves are hand drawn to fit points averaged every 5° west of 15°W and every 2° east of 15°W. Nearly identical months are averaged together.

Using the 20°C isotherm depth to represent the thermocline depth we examine next the seasonal variations of its zonal structure (Fig. 5). The figure extends to the west in order to compare thermal variations within the Gulf of Guinea to those throughout the entire equatorial Atlantic. The data are averaged from 1½°N to 1½°S with zonal averaging over 5° west of 15°W and 2° east of 15°W. The standard deviation about these calculated means is approximately 10 m. The curves in Fig. 5 are hand drawn, averaging together months which are nearly identical. The resulting pattern does not exhibit a simple seasonal "sea-saw" about a pivot point as shown by Merle (1980). In particular during June the thermocline rises in the center of the basin between 35–15°W prior to tilting in July. By averaging April to June and July to September, Merle suppresses some of this variability. As we will show later, June in the Gulf of Guinea is a transition month to which it may not be appropriate to ascribe a climatic mean.

The temporal distribution of the data can seriously distort calculations of a mean temperature structure and results derived from a historical data file must be carefully examined to guard against this. There are two specific problems. First is the limited size of the data file. Most climatic means for any grid point contain data from 2–5 years. Although interannual variability is smaller than the annual signal by a factor of 2–3 and could presumably be averaged out, with such a small sample the particular years incorporated in a

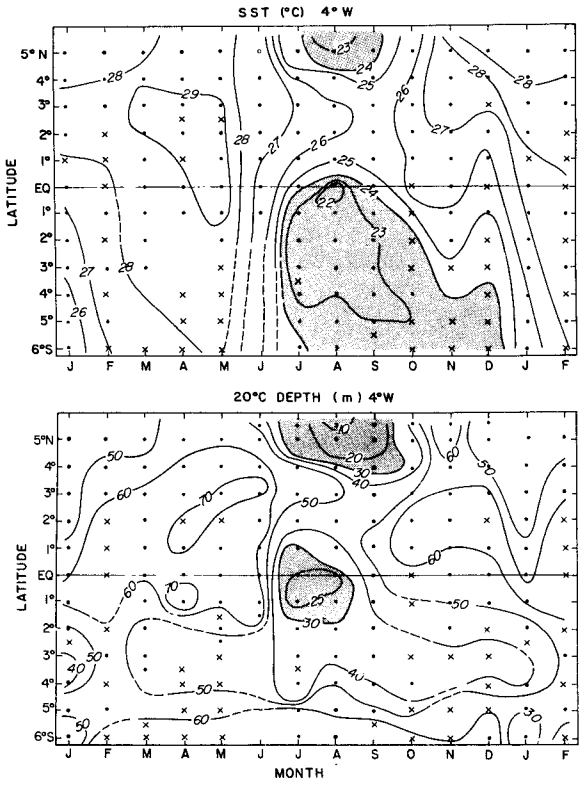

FIG. 6. Monthly mean SST (top) and 20°C depth (bottom) along 4°W versus latitude. The crosses indicate grid points (2° longitude by 1° latitude) with fewer than four stations.

grid point may not represent a "climatic" mean. The second concerns the fact that each station is weighted equally, i.e. considered independent, although upon close examination of the file we often find two or more stations taken at the same location within hours of each other. This could occur when an XBT is deployed at a Nansen station or when, such as during GATE, a ship is anchored for an extended period. What interval is required to make temperature measurements independent? During GATE low-frequency fluctuations with periods of 5–10 days were observed on the equator between 15 and 30°W with vertical displacements equal in magnitude to the seasonal signal. Fortunately the GATE data were of sufficient density and duration to average out these fluctuations, but other data could be seriously aliased by these low-frequency fluctuations.

Some of these sampling difficulties are illustrated in Fig. 5. The monthly averages are never calculated with data from more than five different years, and there is no month for which data from a single year span the entire equator. Thus some of the apparent zonal structure may arise from interannual variability. The curve for June is particularly interesting for it appears that the rise in the thermocline in the middle of the basin (30–15°W) and at the eastern boundary precedes the rise at the center of the Gulf of Guinea (0–10°W) or the fall at the western boundary. The June data derived predominantly from the year 1975 in the west, 1974 between 25 and 15°W, 1968 between 10 and 3°W, and 1964 in the east. Therefore, although the change in thermocline depth between 20 and 5°W exceeds twice the standard deviation about the calculated means, this structure could reflect the fact that 1974 was a "normal" cold season while 1968 was anomalously warm throughout the Gulf of Guinea (Merle *et al.*, 1979). Unfortunately the GATE field program began in June so there is no data between 15 and 24°W in May for comparison. In order to minimize these problems we will focus our attention on the region between 3 and 5°W where the data are most dense and, except for June, are distributed over a number of years.

In Fig. 6 we compare the SST and 20°C depth on a latitude versus time plot along 4°W from 6°S to the coast at 5°N. The crosses denote grids containing fewer than four stations. Occasionally where data density is rapidly changing the grid point is calculated every $\frac{1}{2}$° latitude. The dashed lines indicate regions where the contouring is particularly subjective because of sparse data.

SST and 20°C (thermocline) depth are highly correlated at the equator and the coast. In contrast, south of 4°S the annual signal in the SST persists, but with little change in thermocline depth. Presumably the cold SST south of the equator is the result of advection of cold water from the eastern boundary by the SEC. Thus the meridional asymmetry about the equator seen in the SST maps during August (Fig. 1) does not reflect the underlying thermal structure for the thermocline depth is symmetric about the equator.

The vertical displacement at the equator extends down through the water column. In Fig. 7 we show the time series of the monthly-mean depth of various isotherms averaged over the internal 3 to 6°W and $1\frac{1}{2}$°N to $1\frac{1}{2}$°S. The standard deviation about the mean is approximately 15 m. Down to 300 m depth a seasonal signal in the isotherm depth is discernible. Given the limited temporal resolution there is no apparent vertical phase propagation of this signal. Gouriou (1982), using a slightly larger data file, obtained similar results.

In order to examine this seasonal signal at the equator in more detail the depth of 20°C versus time is shown in Fig. 8. The solid line is the same monthly mean used in Fig. 7. Unlike the western equatorial Atlantic (Fig. 4) where the seasonal variation in thermocline depth is dominated by the annual cycle (Merle *et al.*, 1979; Garzoli and Katz, 1983; Merle and Delcroix, 1984), in the Gulf of Guinea higher harmonics contribute to a semi-annual variation. In Fig. 8 the mean thermocline depth appears to be bimodal, remaining essentially constant throughout the year except when it shoals rapidly in July and August. The abrupt rise between June and July is surprising since the time

of the wind intensification throughout the equatorial Atlantic (from the file of the late A. F. Bunker, courtesy E. Katz) has an interannual variation of several months, and one would expect that the climatic mean of the response to this wind forcing would also be spread out over several months.

To examine the effect of interannual variability, the data are partitioned by year. The individual symbols in Fig. 8 represent averages spanning up to four days and, therefore, are relatively more independent and equally weighted than the individual stations in the historical file. In addition we have added data from the French sections at 4°W CIPREA (courtesy of the French CIPREA group) and U.S. SEQUAL XBT sections at 9°W (courtesy J. Bruce) for the years 1978–81.

Figure 8 now reveals several interesting features about the data distribution. First we note that in the historical file the June and July data have no years in common. Almost all of the June data are from 1968 which were anomalously high resulting in a strongly biased mean. During May and June the thermocline is observed both deep and shallow. In 1964 it appears that the rapid shoaling was observed during May. From this we infer that at the equator in the Gulf of Guinea the thermocline shoals rapidly sometime during May and June. A rapid (~ one month) uplifting in the thermal structure has been inferred from inverted echo sounder records in 1980 (Miller, 1981) although it occurred during March. The dashed line is the mean depth calculated from the symbols in Fig. 8 included

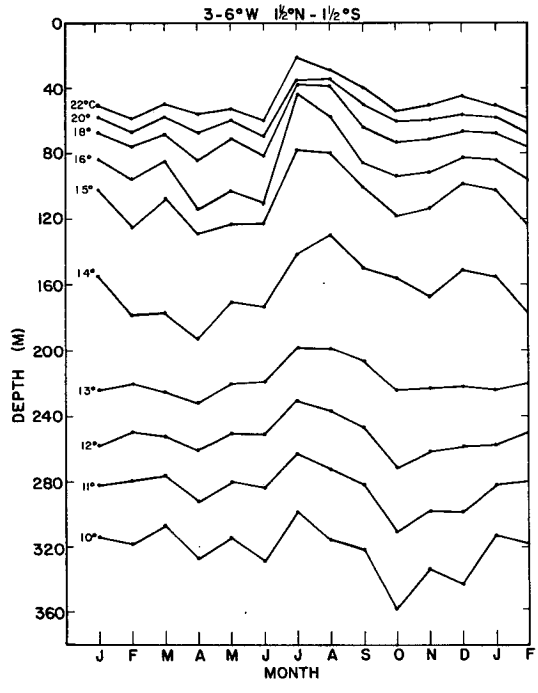

FIG. 7. Monthly mean depth of various isotherms calculated from historical file averaged over 3 to 6°W and 1½°N to 1½°S.

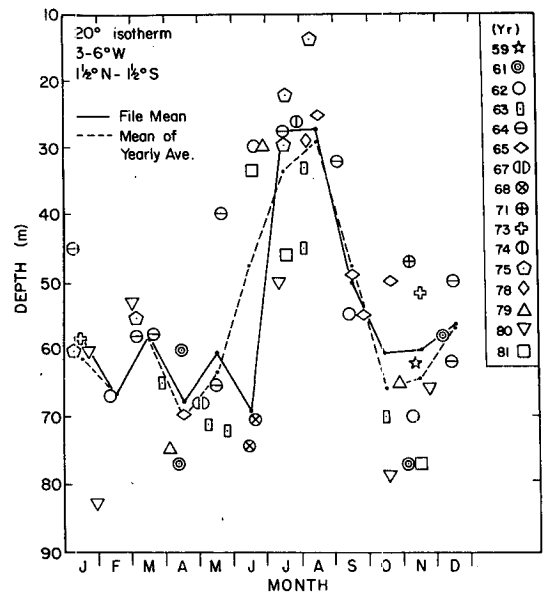

FIG. 8. Annual cycle of 20°C depth, averaged from 3 to 6°W and 1½°N to 1½°S. Solid line, mean of historical data; dashed line, mean of individual yearly averages. The symbols partition the data by year: 1959–75, the historical data with averages up to a four-day interval; 1978–79, CIPREA cross-equatorial sections (courtesy French CIPREA group); 1980–81 SEQUAL XBT sections crossing equator at 9°W (courtesy J. Bruce).

in 1978–81. The two curves are similar except now the shoaling of the thermocline is spread over May and June. The interannual variability of the thermocline depth has an amplitude approximately one half of the seasonal signal. During July and August this variance arises because of differences in the amplitude of the seasonal signal while during June it results from variations in the onset of the seasonal signal. In our subsequent study of the structure of this seasonal signal we will average together the months March–May for the warm season and average July and August for the cold season, omitting June since it is a period of transition.

The meridional structure of the seasonal displacement of the thermocline is calculated in the following way. From the historical file monthly-mean temperature profiles are calculated from 8°S to the coast over a box 1° in latitude bounded by 3°W and 6°W. The depth of 20°C for various months is shown in Fig. 9a. The solid lines represent the mean structure for the warm (March–May) and cold (July–August) seasons. These lines are hand drawn weighing the monthly averages proportionally to their numbers of stations. The difference between these two curves, shown in the bottom panel, is the vertical displacement of the isotherm $h(y)$. As first mentioned by Vioturiez (1981), $h(y)$ is maximum at the equator. So also is the seasonal change in the SST (see Fig. 6), but it remains large to the south of the equator. In contrast $h(y)$ is trapped near the equator.

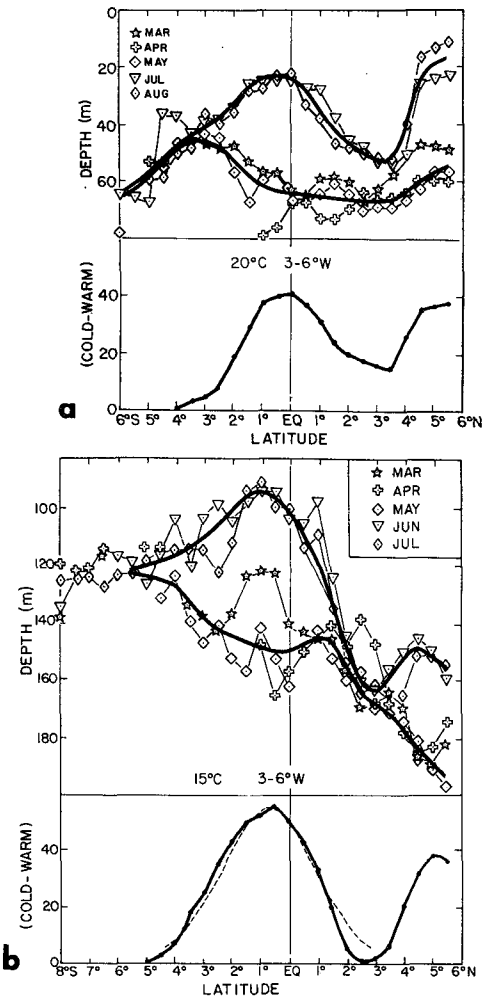

FIG. 9. Climatic meridional sections at 4°W showing depth of (a) 20°C and (b) 15°C. On top, hand-drawn curves average warm season (March–May) and cold season (July–August). Below, the vertical displacement is given by the difference of these two curves with a Gaussian fit (dashed line).

A similar calculation for the 15°C isotherm is shown in Fig. 9b. Here $h(y)$ is even more sharply peaked about the equator with a node at 2½° before increasing at the coast. Near the equator $h(y)$ is well-fitted by a Gaussian curve,

$$h(y) = a_0 \exp\left[\frac{1}{2}\frac{\beta}{c}(y - y_0)^2\right]$$

with $a_0 = 54$ m, $y_0 = 0.75°$S and an e-folding scale

$$\left(\frac{2c}{\beta}\right)^{1/2} = 255 \text{ km}.$$

This is the structure of an equatorially-trapped Kelvin wave with a Rossby radius of deformation $L = (c/\beta)^{1/2} = 180$ km and phase speed $c = 75$ cm s^{-1} for $\beta = 2.3 \times 10^{-11}$ m^{-1} s^{-1}. We will compare this result with other observations and model predictions in Section 4.

In order to construct the vertical structure of the displacement field, the displacement of other isotherms from 22°C to 12°C was calculated. The vertical displacement is assigned to the depth mid-way between the warm and cold season depths of a particular isotherm. The displacement field $h(y, z)$ from 6°S to 6°N along 4°W between 40 m and 240 m depth is shown in Fig. 10. At both the equator and the coast $h(y, z)$ remains large down to 200 m. The maximum displacement, ~60 m, occurs near 160 m at 0.5°S, and there is a node at 2.5°N from 100 m to 140 m. Except for the distortion at 150 m south of 4°S, the e-folding scale (fine dashed line, Fig. 10) is independent of depth.

From similar calculations using the entire historical file we have constructed maps of the topography and displacement field of selected isotherms throughout the Gulf of Guinea (Fig. 11). The crosses denote grid points containing fewer than four stations. In spite of regions with sparse data several distinctive patterns are evident. During the warm season (Fig. 11a, top panel), the topography of the thermocline is relatively flat with a ridge at 3°S. During the cold season (middle panel) thermocline shoaling is greatest in three distinct regions: along the northern boundary between 2°E and 10°W, along the eastern boundary south of 2°S, and on the equator between 0° and 10°W. The map of $h(x, y)$ in the bottom panel accentuates these features. Thermal topography maps at greater depths (Fig. 11b) show a peak in $h(x, y)$ on the equator between 4 and 10°W. Because of sparse data the western extent of this feature is poorly resolved. To the east the reversal in the slope of the zonal temperature gradient (see also Fig. 5) results in a relative minimum in h at 2°E. On

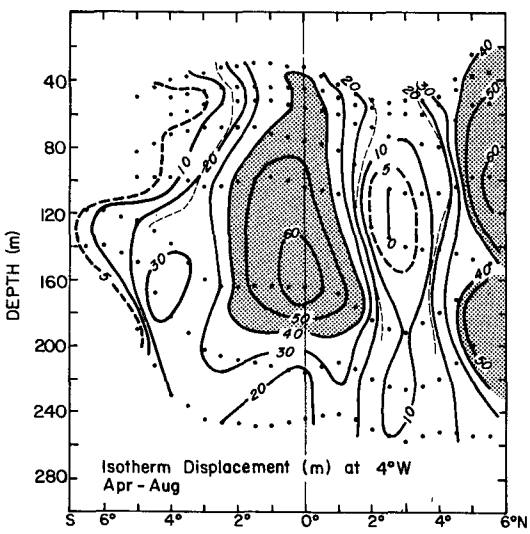

FIG. 10. The vertical displacement field as a function of depth along 4°W across the equator from the coast to 6°S. Locus of e-folding distance shown by fine dashed line.

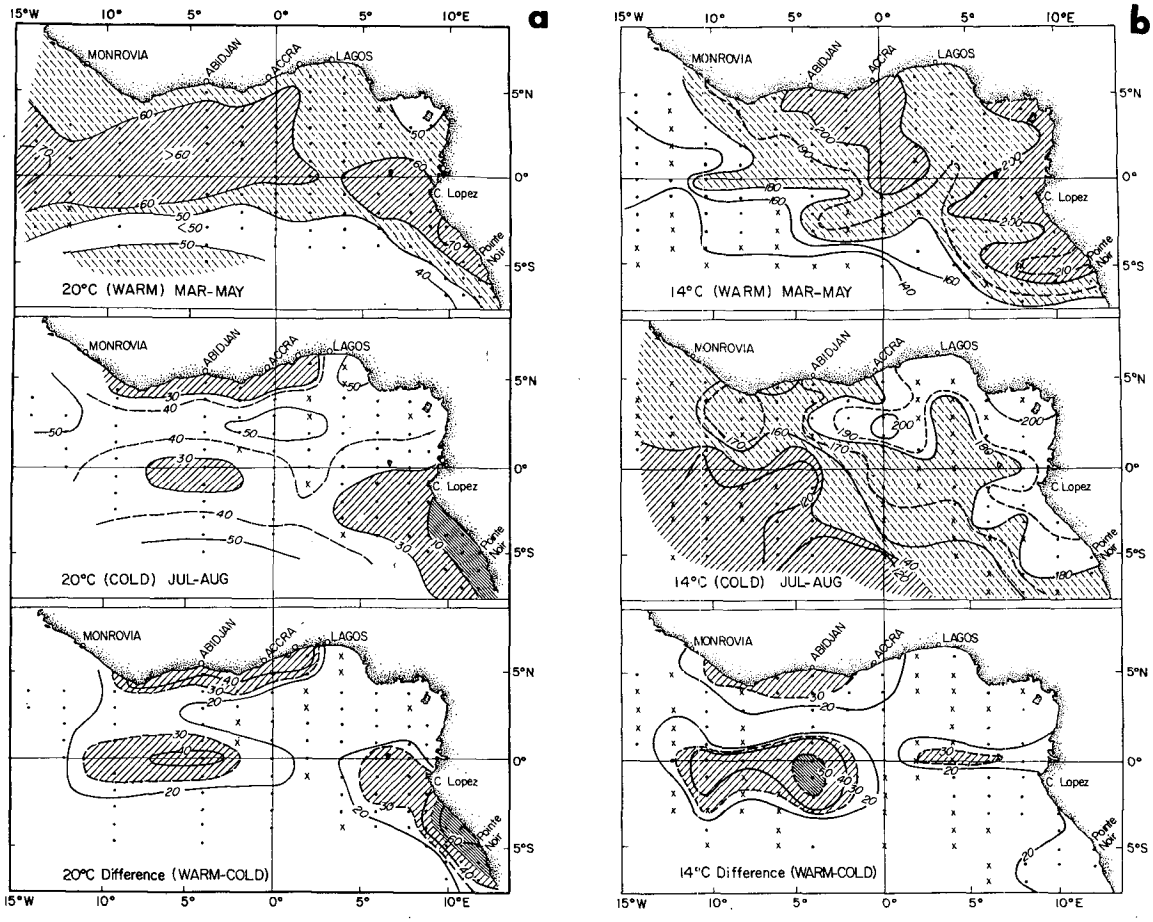

FIG. 11. Average topography of (a) 20°C and (b) 14°C for the (top) warm season and (middle) cold season throughout the Gulf of Guinea. Grid points with fewer than four stations denoted by an x. The vertical displacement field (bottom) is the difference of the upper two.

the eastern boundary south of Cap Lopez h is large near the surface but disappears below 150 m. Along the eastern boundary north of the equator h vanishes until it peaks again between 2°E and 10°W where it persists down to 200 m.

Since the maps in Fig. 11 are constructed from averages over several months we are not suggesting that the thermocline shoaling occurs simultaneously throughout the Gulf of Guinea. It appears to start first during May on the equator west of 10°W and east of 5°E and south of Cap Lopez, then on the equator between 0° and 10°W, and finally along the coast to the north. Until a synoptic data set is available it is impossible to determine more precisely the time lags associated with this sequence.

Enhanced turbulent mixing or divergent flow associated with the EUC can distort the thermal structure at the equator. In Fig. 3 there is a distinct weakening of the thermocline coincident with the core of the EUC. Therefore, it is possible that the observed vertical isotherm displacements reflect fluctuations of the EUC. However, this is not likely. In the Gulf of Guinea there is an annual variation in the velocity of the EUC but not its depth which remains near 60 m (Voituriez, 1981). The isotherm spreading observed in Fig. 3 covers a much smaller region than the displacement field (Fig. 10). Also if isotherm displacement resulted only from changing EUC strength they should be out of phase above and below the core of the EUC. Instead, our results suggest that the equatorially trapped displacement field encompasses an area larger than that influenced directly by the EUC.

4. Discussion

Our objective is to compare our results with other observations and with model predictions. Ultimately one would like to identify the forcing mechanism for the vertical displacements in the Gulf of Guinea.

a. Equatorial response

Evidence for an equatorially trapped wave was first reported by Wunsch and Gill (1976) using tide gauge records from various Pacific islands. Using a coherent

TABLE 1. Scales of baroclinic modes in the equatorial Atlantic. Equivalent depth is h_e, phase speed is $c = gh_e$ and Rossby radius of deformation is $L = (c/\beta)$.

n	h_e (cm)	c ($cm^{-1}s$)	L (km)
1	60	240	325
2	20	140	247
3	8	88	197
4	4	63	165

array of tide gauges in shallow water near the Galápagos Islands at 91°W, Ripa and Hayes (1981) observed low-frequency fluctuations (~100 day) trapped at the equator. Since the meridional structure fitted a Gaussian centered at the equator with an *e*-folding scale of ~490 km the feature was identified as a first baroclinic Kelvin wave. So was a non-dispersive sea level disturbance observed by Knox and Halpern (1982) propagating eastward from the dateline to the Galápagos Islands at a speed of 2.9 m s^{-1}. There is also evidence of an equatorial trapped Kelvin wave from the analysis by Lukas (1981) of the thermal structure in the eastern Pacific. Using mean temperature sections along 92°W the change in depth of the 15°C isotherm from October–December to January–March was fitted to a Gaussian centered at 1°S with an *e*-folding trapping scale of 308 km. This implies a phase speed and equivalent depth of 105 cm s^{-1} and 12 cm, appropriate for a second baroclinic Kelvin wave. These two observations are not necessarily contradictory since sea level variations are more sensitive to the first baroclinic mode (Wunsch and Gill).

In the Atlantic, equatorially trapped Kelvin waves forced by impulsive winds were first suggested by Moore *et al.* (1978) to account for the observed equatorial and coastal upwelling. Using the phase lag between the onset of the equatorial and coastal upwelling in the Gulf of Guinea they inferred a signal propagating eastward with a speed of the order of 2.50 m s^{-1} corresponding to a first baroclinic Kelvin wave (see Table 1). A subsequent reduced gravity model by Adamec and O'Brien (1978) used a phase speed of 1.1 m s^{-1} and radius of deformation ~225 km which corresponds to the second baroclinic mode. In this model the upwelling in the Gulf of Guinea is remotely forced by the impulsive onset of the zonal wind in the western equatorial Atlantic generating a Kelvin wave that propagates eastward then poleward along the eastern boundary.

When the wind forcing is periodic the response is qualitatively different. Cane and Sarachik (1981), who used a pure sinusoidal wind, and Busalacchi and Picaut (1983) and Cane and Patton (1984), who used climatic mean winds to force a linear shallow water model, obtain the seasonal change in the zonal slope of the thermocline along the equator about a pivot point near 20°W. This arises from the superposition of Kelvin and Rossby waves. With low-frequency wind forcing one does not expect to observe a freely propagating Kelvin-wave front in the Gulf of Guinea. These studies also demonstrate that the thermal structure in the Gulf of Guinea responds to wind forcing over the entire equatorial basin.

Calculations of the vertical structure of the ocean response are derived from models with continuous stratification. In their non-linear model Philander and Pacanowski (1980) find that the response of the upper ocean is primarily via the second baroclinic mode which is trapped above the thermocline. In the linear model of McCreary *et al.* (1983) the ocean response is not dominated by any single baroclinic mode but instead is distributed over a number of modes.

We have shown that the meridional structure of the vertical displacement field h along 4°W suggests an equatorially-trapped Kelvin wave. Its radius of deformation ~255 km implies a phase speed $c = \beta L^2 = 75$ cm s^{-1} and an equivalent depth $h_e = c^2/g \sim 6$ cm and this roughly corresponds to the third baroclinic mode (see Table 1). This is consistent with the vertical structure shown in Fig. 12 where $h(z)$ at 0°N, 4°W is compared with the first four modes of a free standing wave calculated using the mean stratification in the Gulf of Guinea (S. Garzoli, personal communication, 1983). The displacement field is maximum below the thermocline at 180 m. The observed structure falls somewhere between the second and third mode although below 180 m h decreases much more abruptly than for any other single mode. Although there is no reason to assume that a modal description is applicable,

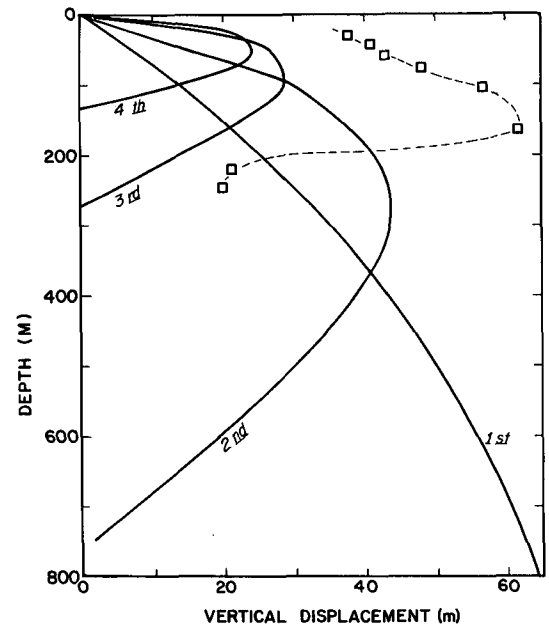

FIG. 12. Vertical structure of the displacement field on the equator at 4°W. Solid curves are the first four baroclinic modes calculated from annual mean stratification (courtesy, S. Garzoli).

the vertical and meridional scales of the displacement field are clearly shorter than those expected for the first baroclinic Kelvin wave.

We have no direct evidence that this equatorially trapped feature is the response to a freely propagating Kelvin wave generated in the western equatorial Atlantic. If that were the case, we would expect h to have a constant amplitude along the equator and not the zonal structure shown in Fig. 11. Also the time lag between the onset of the zonal winds in the western Atlantic and the response in the Gulf of Guinea appears to be too short for Kelvin wave propagation. In 1979 the wind recorded continuously from St. Peter and St. Paul Rocks at 0°55'N and 29°21'W (Garzoli *et al.*, 1982), increased suddenly during mid-May. A second-mode baroclinic Kelvin wave generated by this impulsive forcing would arrive in the Gulf of Guinea a month after the observed upwelling response.

As we have noted, the seasonal fluctuation of the zonal tilt of the thermocline along the equator (Fig. 5) does not exhibit a simple "see-saw" motion about a fixed pivot point as previously reported by Merle (1980) and modeled by Cane and Sarachik (1981), Busalacchi and Picaut (1983) and Cane and Patton (1984). Although longitude 25°W roughly separates the shoaling thermocline to the east from the deepening thermocline to the west, there is no longitude with a distinct minimum in the variance.

In the Gulf of Guinea the equatorially trapped displacement field is not quite symmetric about the equator (see Figs. 6, 7, and 10) but is centered near 0°30'S. A similar asymmetry is observed in the western Atlantic (Garzoli and Katz, 1983) and the eastern Pacific (Lukas, 1981). This asymmetry suggests that something more than Kelvin waves forced by zonal wind stress is involved. Forcing by the meridional wind stress, which in the Gulf of Guinea exceeds the zonal wind in both the mean and the annual variation (Busalacchi and Picaut, 1983), could be involved.

The response to meridional forcing at the equator has been modeled by Philander (1979), Cane (1979), Anderson (1979) and Philander and Pacanowski (1981). The temperature field derived by Philander (1979) using meridional wind stress and a northern boundary to simulate the Gulf of Guinea shows a broad shoaling of the thermocline south of the equator and a downwelling at 3°N. This shoaling could be responsible for the thermal ridge centered at 3°S during the warm season (Voituriez, 1981) which is evident in Figs. 9 and 11. However, north of the equator we observe shoaling of the entire thermal field except for the node at 3°N. In addition the distortion of the model thermal field (Philander, 1979) does not penetrate below 100 m while we observe (Fig. 10) a seasonal signal below 200 m. Although the local meridional wind undoubtedly influences the response in the Gulf of Guinea it does not appear to be dominant.

There is one feature in our results that is absent from all the models that we have referenced. During July and August (Fig. 5) the zonal tilt of the thermocline along the equator reverses between 0° and 4°W. This results in a maximum in the displacement field between 4°W and 10°W and a node near 2°E (Fig. 11). Although the data are sparse especially south of the equator and the calculations are always liable to bias from interannual variability, the same feature, though weaker, is evident in data from 1964 and CIPREA II (June–July, 1979).

As noted by Weisberg and Tang (1983), there are several other features that are particular to the western Gulf of Guinea. This is a region of maximum SST variability which presumably is related to the underlying thermocline fluctuations. It is also the region where the zonal wind stress changes sign. Using a mean surface wind field computed by Hastenrath and Lamb (1977), Busalacchi and Picaut (1983) show that the locus of zero zonal stress is a line across the Gulf of Guinea from southeast to northwest crossing the equator at 4°W. Using the same data, Picaut (1983) presents the longitudinal structure of the seasonal evolution of the zonal wind stress and shows that the intensification of the westward stress first begins in April between 0° and 10°W and then moves westward. Weisberg and Tang have simulated this forcing by modeling the response of a two-layer reduced-gravity model forced by zonal winds with constant and intensifying winds with a fetch growing linearly to the west. Their results, a superposition of Kelvin and Rossby waves, produce a vertical displacement which is maximum at the longitude where the zonal wind originates; in the Gulf of Guinea this is near 5°W.

No other model has produced a similar result. Since Busalacchi and Picaut (1983) used the Hastenrath and Lamb (1977) wind field and realistic topographic boundaries, one might expect to see this feature in their results. Except for a faint trace in their Fig. 7 none is evident. This might arise from the fact that they decomposed the wind field into harmonic components and the resulting spatial and temporal smoothing may eliminate the impulsively generated wave field modeled by Weisberg and Tang (1983).

It seems increasingly clear that the representation of the wind field critically affects model results especially in the Gulf of Guinea where both local and nonlocal forcing appear to be important. Although the seasonal variation of the climatic wind field is dominated by the lower-harmonic components (Picaut, 1983), individual yearly records such as 1979 on St. Peter and St. Paul Rocks (Garzoli *et al.*, 1982) often show rapid changes that are more akin to impulsive wind forcing. Use of climatic winds in which such impulsive features are averaged out may not be sufficient to model the ocean response. A synoptic wind field of the entire equatorial Atlantic for a particular year is required to model the response in the Gulf of Guinea.

b. Coastal response

The existence of the coastal upwelling in the Gulf of Guinea is clearly evident in SST data (Fig. 1). The band of low SST along the northern boundary is distinct from the equatorial upwelling and is correlated with local thermocline displacements (Fig. 6). In spite of the initial attempt by Ingham (1970) to evaluate the role of local wind and currents, the forcing mechanism for this upwelling has never been clearly identified. Houghton (1976) and Bakun (1978) failed to find a correlation between the upwelling and local coastal winds which have a very weak seasonal variation. Direct calculations of Ekman divergence by Verstraete (1970) give vertical velocities much smaller (8.1×10^{-6} m s^{-1} or 0.7 m day^{-1}) than observed (Houghton, 1976).

The situation is similar along the coast south of the equator. Although Philander and Pacanowski (1981) have modeled the generation of low SST by a local meridional wind stress and its westward expansion by advection and Rossby wave propagation, the climatic winds (Hastenrath and Lamb, 1977; and Picaut, 1983) show little seasonal variation along the coast north of 15°S. Consequently Berrit (1976) and Picaut (1983) found little correlation between local winds and nearshore SST variations north of 15°S.

Lacking an obvious local forcing mechanism, nonlocal forcing becomes more attractive. The initial idea (Moore *et al.*, 1978) of an impulsively forced Kelvin wave that propagates freely across the Gulf of Guinea and then poleward along the eastern boundary has been superceded by models with more realistic wind forcing (Busalacchi and Picaut, 1983; McCreary *et al.*, 1983) in which the response is a suerposition of Kelvin and reflected Rossby waves.

Our analysis (Fig. 11) shows that along various portions of the coast the response is distinctly different. South of Cap Lopez the vertical displacement of the thermocline is greatest. However, the displacement field does not extend below 150 m. Were it not for the lack of correlation with the wind one might assume that this was a locally forced coastal upwelling.

North of the equator along the Nigerian coast the displacement field is absent at all depths. Although the data are sparse in this region, hydrographic sections taken across the shelf south of Lagos during 1961 and 1962 and reported by Longhurst (1964) are instructive. They show a seasonal fluctuation in the SST from 28 to 24°C associated with changes in the stratification in the upper layer but with less than a 20 m displacement in the 20°C isotherm which is located within the thermocline. The thermocline depth is constant across the section which extends to 46 km offshore, well beyond the shelf break.

On the northern boundary of the Gulf of Guinea the vertical displacement field (Fig. 11) is trapped along the coast from 2°E to 10°W in much the same way as the band of low SST (Fig. 1). The displacement field extends down to 220 m (Fig. 10) and has an *e*-folding scale of approximately 160 km at all depths. Associating this with a coastal Kelvin wave with an internal Rossby radius of deformation $L_c = c/\beta y$ and with $y = 500$ km we get a phase speed $c = 1.7$ m s^{-1}. This inferred phase speed is nearly twice the westward propagation speed of the seasonal coastal upwelling inferred by Picaut (1983) from SST data.

A clear understanding of the forcing mechanisms responsible for this coastal upwelling is made difficult because of the potential influence of a number of local factors. First, the local wind has a direction that is favorable to upwelling but is weak. The amplitude of the SST change during the upwelling is greatest east of Cape Palmas at 8°W and Cape Three points at 2°W (Picaut, 1983). This could arise from the more favorable orientation of the coastline with respect to the local wind in addition to the influence of the Cape on the coastal currents. Finally there is the geostrophic adjustment of the density field to the eastward Guinea Current. Its seasonal variation has been reported by Janke (1920), Ingham (1970), Bakun (1978) and Hisard and Merle (1979). Philander (1979) has shown how this could arise from the seasonal intensification of the cross-equatorial winds. However, data are too sparse to resolve in detail the relation between the intensity and structure of this current to the coastal upwelling.

What then is the connection between the coastal and equatorial upwelling? The meridional scale lengths of each are sufficiently short that the two regimes are separate and distinct. Of particular interest is the time lag in the onset of the upwelling at the two locations. It was an estimate of this lag during GATE in 1974 that led to the simple Kelvin waves model of upwelling in the Gulf of Guinea (Moore *et al.*, 1978). A close inspection of the GATE data (Bubnov *et al.*, 1979) shows that the SST data were in this case misleading. The observed drop in the equatorial SST at 10°W in July was really accompanied by a drop not a rise in the thermocline depth and the onset of the seasonal upwelling probably occurred earlier (before the GATE field program started).

The suggestion of a time lag between the onset of the upwelling at the coast and equator is barely discernable in the climatic mean. In Fig. 6 we see that the thermocline shoals in July and August at the equator and in August and September at the coast. Data from individual years are usually too sparse for adequate temporal resolution of the upwelling event. Only in 1964 is it clear that the equatorial upwelling precedes the coastal upwelling by approximately one month.

The apparent isolation of this coastal upwelling from the equatorial regime renews the possibility that it is coastally generated, not locally, but to the east along the coast of Nigeria. Clarke (1979) presented such a model and by projecting winds measured at Lagos (3°30′E) during 1974 along the eastern boundary pro-

duced a sea level response at Tema (0°W) that is qualitatively similar to observations although considerably smaller. Without more realistic coastal winds and more precise measurements of the alongshore propagation and dissipation it is not clear whether this discrepancy is significant.

5. Conclusion

In spite of the limitations imposed by the distribution of the historical data file, our analysis has revealed several distinctive features in the subsurface thermal structure in the Gulf of Guinea. The vertical displacement of the water column in response to the seasonal wind forcing occurs rapidly (one month) and is trapped about the equator with vertical and meridional scales appropriate to a second or third baroclinic Kelvin wave. The maximum response occurs between 0°W and 10°W. South of 4°S there is no thermocline displacement associated with the annual SST variation. Along the coast there is a seasonal displacement of the thermocline everywhere except north of the equator along the Nigerian coast to 2°W.

Each of these features appears among the various models of the Gulf of Guinea response to wind forcing, but no single model does it all. The models do show that the Gulf of Guinea response depends on the wind field throughout the equatorial Atlantic and the model results are sensitive to how the spatial and temporal structure of this wind is represented. Two situations have yet to be modeled: the response to an annual impulsive wind event and a nonlinear ocean forced by climatological winds. However, climatic wind fields may obscure important features in the actual forcing field. In the same way, mean thermal structure derived from these historical hydrographic data obscures the detailed structure and phase lags of the response. Only a synoptic data set of both the wind and ocean structure during a single annual cycle (now being generated by the ongoing SEQUAL–FOCAL field program) will show clearly the ocean response to wind forcing and critically test the prevailing model calculations.

Acknowledgments. The initial data used in this study were kindly provided by Jacques Merle. The author acknowledges the computational assistance of P. Mele and the sugggestions and stimulating conversations with SEQUAL and FOCAL participants. This work was supported by National Science Foundation Grant OCE 79-23632 and OCE 81-17554.

REFERENCES

Adamec, D., and J. J. O'Brien, 1978: The seasonal upwelling in the Gulf of Guinea due to remote forcing. *J. Phys. Oceanogr.*, **8**, 1050–1060.

Anderson, D., 1979: Low latitude seasonal adjustment in the Atlantic, (unpublished manuscript).

Bakun, A., 1978: Guinea Current upwelling. *Nature*, **271**, 147–150.

Berrit, G. R., 1976: Les eaux froides côtieres du Gabon a l'Angola sont-elles dues a un upwelling d'Ekman? *Cah. ORSTOM*, Ser Oceanogr., **14**, 273–278.

Bubnov, V. A., V. D. Egorikhin, F. N. Matveeva, S. E. Navrotskaya and D. I. Filippov, 1979: Graphical presentation of the USSR oceanographic observations in the tropical Atlantic during GATE (June to September, 1974). RSMAS/University of Miami, Tech. Rep. TR-79-1; 163 pp.

Busalacchi, A. J., and J. Picaut, 1983: Seasonal variability from a model of the tropical Atlantic Ocean. *J. Phys. Oceanogr.*, **13**, 1564–1588.

Cane, M. A., 1979: The response of an equatorial ocean to simple wind stress platforms: II. Numerical results. *J. Mar. Res.*, **37**, 253–299.

——, and E. S. Sarachik, 1981: The response of a linear equatorial ocean to periodic forcing. *J. Mar. Res.*, **39**, 651–693.

——, and R. Patton, 1984: A numerical model for low frequency equatorial dynamics. Submitted to *J. Phys. Oceanogr.*

Citeau, J., B. Piton and B. Voituriez, 1981: Remote sensing of the upwelling season in the eastern tropical Atlantic Ocean. Rep. Final Meeting of SCOR WG47. Nova University Press, 283–292.

Clarke, A. J., 1979: On the generation of the seasonal coastal upwelling in the Gulf of Guinea. *J. Geophys.Res.*, **84**, 3743–3751.

Garzoli, S., and E. Katz, 1983: The forced annual reversal of the Atlantic North Equatorial countercurrent. *J. Phys. Oceanogr.*, **13**, 2082–2090.

——, ——, H. J. Panitz and P. Speth, 1982: *In situ* wind measurements in the equatorial Atlantic during 1979. *Oceanol. Acta*, **5**, 281–288.

Gouriou, Y., 1982: Etude des variations thermiques sur une annee moyenne dans le Golfe de Guinee a 4°W, entre Abidjan (5°N) et 10°S de 0 a 250 m. Rapport de DEA. Universite de Bretagne Occidentale, 43 pp.

Hastenrath, S., and P. J. Lamb, 1977: *Climatic Atlas of the Tropical Atlantic and Eastern Pacific Ocean.* The University of Wisconsin Press, 15 pp., 97 charts.

Hisard, P., and J. Merle, 1979: Onset of summer surface cooling in the Gulf of Guinea during GATE. *Deep-Sea Res.*, (GATE Suppl. II to V), **26**, 325–341.

Houghton, R. W., 1976: Circulation and hydrographic structure over the Ghana Continental Shelf during the 1974 upwelling. *J. Phys. Oceanogr.*, **6**, 910–924.

——, 1981: Temperature variations in the Gulf of Guinea. *Trop. Ocean. Atmos. News.*, **8**, 1–3 (unpublished manuscript).

Ingham, M. C., 1970: Coastal upwelling in the northeastern Gulf of Guinea, *Bull. Mar. Sci.*, **20**, 1–33.

Janke, J., 1920: Stromungen and oberflachentemperaturen in Golfe von Guinea. *Arch. Dtsch. Seewarte*, **6**, 1–68.

Katz, E. J., and collaborators, 1977: Zonal pressure gradient along the equatorial Atlantic. *J. Mar. Res.*, **35**, 293–307.

Knox, R. A., and D. Halpern, 1982: Long range Kelvin wave propagation of transport variations in Pacific Ocean equatorial currents. *J. Mar. Res.*, **40**, 329–339.

Longhurst, A. R., 1964: The coastal oceanography of western Nigeria. *Bull. Inst. Fr. Afr. Noire*, **26**, 337–401.

Lukas, R. B., 1981: The termination of the Equatorial Undercurrent in the eastern Pacific. Ph.D. dissertation, University of Hawaii, 127 pp.

McCreary, J. P., J. Picaut and D. W. Moore, 1983: Effect of annual remote forcing in the eastern tropical Atlantic. *J. Mar. Res.* (in press).

Merle, J., 1980: Seasonal heat budget in the equatorial Atlantic Ocean. *J. Phys. Oceanogr.*, **10**, 464–469.

——, 1983: Seasonal variability of subsurface thermal structure in the tropical Atlantic Ocean. *Mem. Soc. R. Sci. Liege*, J. Nihoul, Ed., 6e Ser, **14**, (in press).

——, and T. Delcroix, 1984: Seasonal variability of the thermocline topography in the tropical Atlantic Ocean. Submitted to *J. Phys. Oceanogr.*

——, M. Fieux and P. Hisard, 1979: Annual signal and interannual anomalies of sea surface temperature in the Eastern Equatorial Atlantic Ocean. *Deep-Sea Res.*, (GATE Suppl. II to V), **26,** 77–101.

Miller, L., 1981: Acoustic measurements of dynamic height and wind speed in the eastern equatorial Atlantic. Rep. Final Meeting of SCOR WG47, Nova University Press, 325–334.

Moore, D., H. Philippe, J. McCreary, J. Merle, J. O'Brien, J. Picaut, J-M. Verstraete and C. Wunsch, 1978: Equatorial adjustment in the eastern Atlantic. *Geophys. Res. Lett.*, **5,** 637–639.

Philander, S. G. H., 1979: Upwelling in the Gulf of Guinea. *J. Mar. Res.*, **37,** 23–33.

——, and R. C. Pacanowski, 1980: The generation of equatorial currents. *J. Geophys. Res.*, **85,** 1123–1136.

——, and ——, 1981: The oceanic response to cross-equatorial winds. *Tellus,* **33,** 201–210.

Picaut, J., 1983: Propagtion of the seasonal upwelling in the eastern equatorial Atlantic. *J. Phys. Oceanogr.*, **13,** 18–37.

Ripa, P., and S. P. Hayes, 1981: Evidence for equatorial trapped waves at the Galapagos Islands. *J. Geophys. Res.*, **86,** 6509–6516.

Servain, J., J. Picaut and J. Merle, 1982: Evidence of remote forcing in the equatorial Atlantic Ocean. *J. Phys. Oceanogr.*, **12,** 457–463.

Verstraete, J. M., 1970: Etude quantitative de l'upwelling sur le plateau continental ivoirien. Doc. Sci. Centre Rech. Oceanogr., Abidjan, **1,** 1–17.

Voituriez, B., 1981: The equatorial upwelling in the eastern Atlantic Ocean. Rep. Final Meeting of SCOR WG47. Nova University Press, 229–247.

Weisberg, R. H., and D. Tang, 1983: Equatorial Atlantic response to growing and moving wind systems. *J. Mar. Res.*, **41,** 461–486.

Wunsch, C., and A. E. Gill, 1976: Observations of equatorially trapped waves in Pacific sea level variations. *Deep-Sea Res.*, **23,** 371–390.